引用格式：YANG Nana，FANG Bo，WANG Chunhui，et al. Wavelength Modulation Off-axis Integrated Cavity Output Spectroscopy for High-sensitivity Detection of OH Radicals in Mid-infrared[J]. Acta Photonica Sinica，2023，52(3)：0352123
杨娜娜，方波，王春晖，等. 中红外波长调制离轴积分腔输出光谱技术应用于OH自由基高灵敏度探测研究[J]. 光子学报，2023，52(3)：0352123

中红外波长调制离轴积分腔输出光谱技术应用于OH自由基高灵敏度探测研究

杨娜娜[1,2]，方波[1]，王春晖[1,3]，周昊[1,2]，韦娜娜[1]，赵卫雄[1]，张为俊[1,3]

（1 中国科学院合肥物质科学研究院 安徽光学精密机械研究所，合肥 230031）

（2 中国科学技术大学，合肥 230026）

（3 中国科学技术大学 环境科学与光电技术学院，合肥 230026）

摘 要：将波长调制技术与离轴积分腔技术相结合，建立了波长调制离轴积分腔输出光谱实验装置，增加吸收光程，避免低频的1/f噪声和与波长无关的背景功率的影响，将其应用于OH自由基探测研究。探测激光器选择2.8 μm中红外室温型连续波分布反馈式二极管激光器，OH自由基选择3 568.52 cm^{-1}处Q(1.5e)跃迁谱线开展光谱探测，在512 m有效吸收光程和100 s采样时间下，实现了OH自由基1.2×10^{8} $molecule/cm^{3}$的探测极限。实验研究发现，在弱透过光强下，激光器放大的自发辐射对吸收系数测量影响大，本实验装置下造成了约70倍的吸收低估，需要有效避免。

关键词：激光吸收光谱；中红外；离轴积分腔；放大的自发辐射；OH自由基

中图分类号：O433.4 **文献标识码**：A **doi**：10.3788/gzxb20235203.0352123

0 引言

1998年，ENGELN R等[1]通过调谐激光波长，测量透过谐振腔的光强而非衰荡时间来进行光谱探测，降低了在腔衰荡光谱(Cavity Ring Down Spectroscopy，CRDS)[2]技术中对探测器电子带宽的需求，该技术被命名为腔增强吸收光谱(Cavity Enhanced Absorption Spectroscopy，CEAS)技术。同年，O'KEEFE A等[3-4]在调谐激光波长的同时，在腔镜上增加压电陶瓷以周期性改变腔长，对透过谐振腔的积分光强进行探测，称之为积分腔输出光谱(Integrated Cavity Output Spectroscopy，ICOS)技术。

为了进一步减小谐振腔干涉效应带来的光强波动噪声，2001年，PAUL J B等[5]提出采用离轴入射的方式让激光进入谐振腔，主动激发出许多不同阶数的横模，降低基模与高阶模的强度差异，使得输出光谱更加连续与平滑，标志着离轴积分腔输出光谱(Off-axis Integrated Cavity Output Spectroscopy，OA-ICOS)技术正式诞生。OA-ICOS技术周期性破坏腔的共振，实现了腔对激光频率的平均透过，透射光谱接近于传统的直接吸收光谱。因此在直接吸收光谱中所使用的调制方法及灵敏度表示方法均适用于OA-ICOS。随后，研究者们通过使用大尺寸腔镜[6]来提高激光入射的离轴量，以及给激光器注入射频白噪声[7]来降低激光相干性等方法，进一步减小残余腔模式波动带来的光强噪声。OA-ICOS具有灵敏度高、结构简单、抗环境干扰能力强等优点，广泛应用于大气环境探测[8-9]、呼吸气体诊断[10-11]、同位素分析检测[11-12]等研究领域。

波长调制光谱(Wavelength Modulation Spectroscopy，WMS)技术对激光波长进行高频调制(约1～100 kHz，小于激光线宽)，检测通过样品后的透射光随波长的变化量，再结合锁相放大器解调得到样品的吸

基金项目：国家自然科学基金(Nos. 42022051，41627810)，中国科学院青年创新促进会(No. Y202089)，中国科学院合肥物质科学研究院院长基金(Nos. YZJJ202101，BJPY2019B02)

第一作者：杨娜娜，yn19950121@163.com

通讯作者：赵卫雄，wxzhao@aiofm.ac.cn

收稿日期：2022-05-25；**录用日期**：2022-06-21

收信息，将频谱信号移到高频处测量，有效避免了低频的1/f噪声和与波长无关的背景功率的影响，探测灵敏度比直接吸收光谱方法提升数十倍。2002年，KASYUTICH V L等[13]将波长调制应用于OA-ICOS技术，测量了687 nm处的氧气，在110 m有效吸收光程下获得了1.7×10^{-10} cm^{-1} Hz$^{-1/2}$的等效噪声灵敏度。ZYBIN A等[14]使用波长调制离轴积分腔技术（Wavelength Modulation Off-axis Integrated Cavity Output Spectroscopy，WM-OA-ICOS）测量了833 nm处的碳原子，在8.8 km有效吸收光程下获得了8×10^{-13} cm^{-1} Hz$^{-1/2}$的等效噪声灵敏度。随后BAKHIRKIN Y A等[15-16]在5 μm处对NO进行了测量，证明WM-OA-ICOS技术的探测灵敏度优于OA-ICOS技术，并在约700 m有效吸收光程下获得了一氧化氮（NO）优于1 ppb（10^{-9}）的探测限。ZHAO Weixiong等[17]在1.57 μm处对环境空气中二氧化碳（CO_2）进行探测，在68 m有效吸收光程下得出WM-OA-ICOS的等效噪声灵敏度为3.3×10^{-11} cm^{-1} Hz$^{-1/2}$。2017年，WU Tao等[18]对1.39 μm处的甲烷（CH_4）进行探测，在300 m有效吸收光程下获得了7.3×10^{-11} cm^{-1} Hz$^{-1/2}$等效噪声灵敏度。

羟基（OH）自由基是大气中最重要的氧化剂，在挥发性有机化合物（Volatile Organic Compounds，VOCs）和其他痕量气体的降解过程中起着至关重要的作用[19]，在大气中与过氧化氢（HO_2）自由基、氮氧化物（NO_x，NO_x=NO+NO_2）的链循环转化过程直接影响二次有机气溶胶、酸雨及臭氧的生成[20]。大气中OH自由基浓度极低（$\sim10^6$ molecule/cm^3）、反应活性高、寿命短（<1 s）[21-22]。长期以来，利用激光光谱技术直接测量大气中的OH自由基浓度一直是一个目标，当前仅有基于低压扩散的激光诱导荧光技术（Fluoresence Assay with Gas Expansion，FAGE）[23]和长程差分吸收光谱技术（Differential Optical Absorption Spectroscopy，DOAS）[24]两种激光光谱法能应用于实际大气OH自由基测量，但由于FAGE和DOAS均使用紫外激光光源，存在OH次生，不可避免地受到化学干扰。而红外吸收光谱法，特别是中红外区域，为分子指纹区域，光谱选择性好，吸收干扰小，谱线强度高，对于OH自由基测量具有重要应用前景[25]。。

本文发展了一套用于OH自由基直接探测的2.8 μm中红外波长调制离轴积分腔装置，使用2f谐波探测在100 s积分时间下获得1.2×10^8 molecule/cm^{3}的探测极限。离轴积分腔技术与波长调制技术相结合为OH自由基提供了一个新的直接光谱探测手段，可为后续继续发展OA-ICOS技术与更高灵敏度技术结合，如频率调制技术、磁旋转光谱技术直接探测OH自由基提供参考。

1 原理

在OA-ICOS中，激光偏离几何光轴耦合至高精细度腔内，在满足重入射条件下[26]$2m\theta=2n\pi$，即光束经过m次反射后，再次与第一束入射光重合，其中n为整数，θ为同一个镜面上相邻两个点之间的夹角，可表示为$\cos\theta=1-d/r$，d为腔长，r是腔镜曲率半径。此时谐振腔的自由光谱区范围（Free Spectral Range，FSR）减小为原来的$1/m$倍，当m足够大时，FSR足够小，模式密度增大，谐振腔的透过近似于连续的光谱，透过光强为

$$I=I_0\frac{(1-R^2)\exp(-\alpha(\nu)d)}{1-R^2\exp(-2\alpha(\nu)d)} \tag{1}$$

式中，I_0为无吸收介质时的透过光强，R为腔镜反射率，$\alpha(\nu)$为频率为ν时的吸收系数。当积分腔内满足弱吸收条件（$\alpha d\ll1-R$）时，$\alpha(\nu)$可近似表示为[27]

$$\alpha(\nu)=\sigma(\nu)N=\frac{1}{d}\left(\frac{I_0}{I}-1\right)(1-R) \tag{2}$$

式中，$\sigma(\nu)$为分子吸收截面，N为分子数浓度。

在WM-OA-ICOS探测时，被调制的激光瞬时频率为[28]

$$\nu(t)=\nu_c+a\cos(\omega t) \tag{3}$$

式中，ν_c为激光器中心频率，a为调制振幅，$\omega=2\pi\nu$为调制角频率。

用式（3）对谱线的线宽进行归一化处理，对应的输出频率为

$$\bar{\nu}(t)=\bar{\nu}_d+b\cos(\omega t) \tag{4}$$

式中，$\bar{\nu}_d=\dfrac{\nu_c-\nu_0}{\Delta\nu/2}$，$b=\dfrac{a}{\Delta\nu/2}$，$\bar{\nu}_d$为归一化的中心频率偏移量，$b$为归一化的调制振幅，即调制系数，$\nu_0$为吸收

峰中心频率，$\Delta\nu$为吸收谱线的线宽。

当调制振幅远远小于吸收谱线线宽时（$b\ll1$），利用锁相放大器，在中心频率附近解调得到的二次谐波同相分量可写为[17-18,29-31]

$$S_{2f}(\bar{\nu}_c,b)\Big|_{b\ll1}\approx-\frac{1}{4}\eta\bar{I}b^2\phi^{(2)}(\bar{\nu}_c)\gamma \tag{5}$$

式中，η为光电转换系数，$\bar{I}$和$\phi^{(2)}(\bar{\nu}_c)$分别为在中心频率$\bar{\nu}_c$处的平均光强和线型函数的2阶导数，$\gamma=S\times L\times N$，L为有效吸收光程，S为吸收谱线线强。

由式（5）知$2f$信号强度与γ成正比，而L、S均为常数，故$2f$信号强度与气体浓度N成正比。通过测量不同分子数浓度下的$2f$信号值可获得它们之间的线性关系。

2 实验装置

离轴积分腔输出光谱实验装置如图1所示，探测激光器选择2.8 μm连续波分布反馈式（continuous wave Distributed Feedback，cw-DFB）激光器（Nanoplus），光功率为2 mW，激光器温度和电流使用LDC501激光控制器（Stanford）精确控制。激光经反射镜耦合进入高精细度谐振腔中，腔长为35.8 cm，腔体由两片直径为25.4 mm、曲率半径为1 m的高反射镜构成（R约为99.99%，中心波长为2 900 nm），水平安装在长宽高为15 cm×15 cm×35 cm的铝合金腔体内。透过谐振腔的光经滤波片滤除激光器放大的自发辐射，最后经过焦距为75 mm透镜聚焦后由探测器（PVI-4TE-3.4，VIGO）接收，探测器的跨阻增益为3×10^5 V/A，探测灵敏度为2×10^{11} cm $Hz^{1/2}$/W。

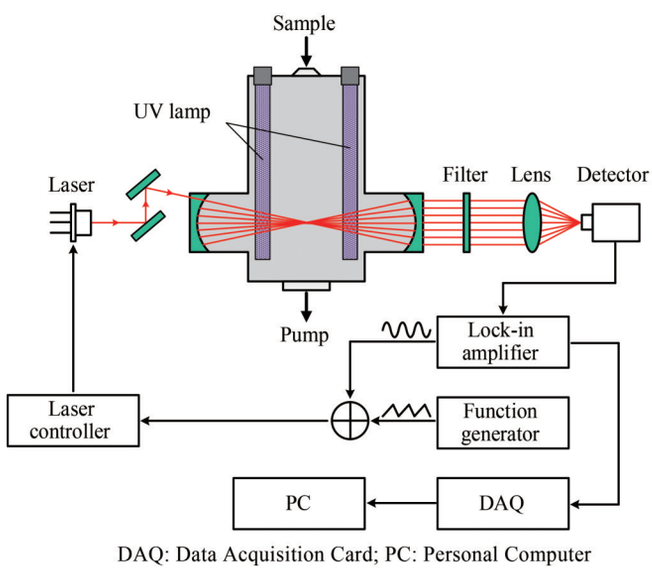

图1 实验装置示意图

Fig.1 Schematic diagram of the experimental setup

使用波长调制离轴积分腔光谱探测时，10 Hz锯齿波和33 kHz正弦波通过加法器（SIM980，Stanford）叠加后送入激光控制器以扫描和调制激光注入电流，OH自由基选择位于3 568.52 cm^{-1}处的Q（1.5e）线（在296 K温度下，线强$S=9.032\times10^{-20}$ $cm^{-1}/(molecule\cdot cm^{-2})$）[32]。探测器接收的光强信号输入至锁相放大器（SR865，Stanford）用于解调二次谐波信号，解调的时间常数为300 μs。

OH自由基在谐振腔内部由254 nm紫外灯光解O_3与水汽发生反应产生[33]。腔内紫外灯开启时，O_3会光解产生激发态氧原子$O(^1D)$，再与水蒸气反应产生OH自由基，其具体化学过程为

$$\begin{cases}O_3+h\nu(<300\text{nm})\rightarrow O(^1D)+O_2\\O(^1D)+H_2O\rightarrow 2OH\end{cases} \tag{6}$$

3 结果与讨论

3.1 放大的自发辐射影响探究

对激光器注入电流时，工作物质在激光器内部的增益介质中获得受激放大，同时也会产生非相干的自发辐射[34-35]，这种放大的自发辐射（Amplified Spontaneous Emission，ASE）会与有效信号互相竞争，增大激光器内部噪声。在一定条件下，一定数量的粒子被激发，产生ASE的粒子数愈多，可用于提供信号增益的粒子数目也就愈少，即ASE会造成反转的粒子数下降，激光增益系数降低。ASE的强度会随激光器注入电流增大而增大，甚至可达到激光发射功率的百分之几[36]，光谱带宽可达几百纳米[37]。

由于离轴积分腔中激光能量被均匀分在密集的高阶模上，最大透过光强仅为耦合到腔内光强的$(1-R)/2$倍，对于反射率为99.99%的高反镜片，仅有入射光的5×10^{-5}能够透过光腔被探测器接收。当激光束经过光腔时，ASE部分直接透过积分腔，与有效信号一起被探测器接收[38]，即

$$\alpha(\nu)=\sigma(\nu)N=\frac{1}{d}\left(\frac{(I_0-I_{\mathrm{ASE}})-(I-I_{\mathrm{ASE}})}{I-I_{\mathrm{ASE}}}\right)(1-R)=\frac{1}{d}\left(\frac{I_0-I}{I-I_{\mathrm{ASE}}}\right)(1-R) \tag{7}$$

式中，I_{ASE}为ASE的透过光强，当有效信号光强大小与ASE强度相当时，将会对吸收系数的测量产生影响。若忽略I_{ASE}，则会导致吸收系数α的低估，进而通过谱线线型反演得到的分子数浓度被低估，影响测量的准确性[39-42]。结果如图2所示，以3 569.55 $\mathrm{cm^{-1}}$附近的CO_2吸收谱线为例，研究ASE对本装置的影响。图2(a)显示出ASE强度受激光功率影响，随激光电流增大而增大，在探测总光强中占比高达97%。将归一化的直接吸收信号使用伏格特（Voigt）拟合，如图2(b)所示，在光路中放置滤光片前后，线型积分吸收由8.1×10^{-6} $\mathrm{cm^{-2}}$提高至5.6×10^{-4} $\mathrm{cm^{-2}}$，即由于ASE影响，积分吸收降低为原来的1/70，导致浓度测量时被低估为原来的1/70。

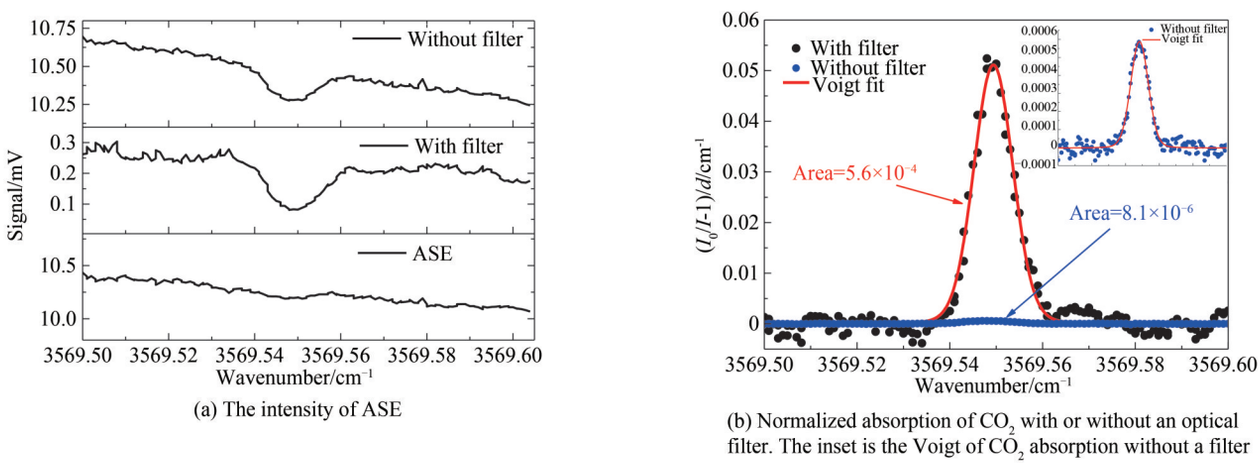

(a) The intensity of ASE

(b) Normalized absorption of CO_2 with or without an optical filter. The inset is the Voigt of CO_2 absorption without a filter

图2 自发辐射放大效应对离轴积分腔输出光谱测量的影响

Fig.2 The effect of ASE on the measurement of OA-ICOS

3.2 WM-OA-ICOS OH自由基测量

离轴积分腔的有效吸收光程L与腔镜有效反射率直接相关，可通过直接吸收拟合已知浓度的气体吸收谱线得到积分面积，进而得到有效反射率R_{eff}[15,43]。实验使用已知浓度CO_2气体在不同压力下的吸收对腔镜有效反射率进行准确标定。CO_2气体选择3 569.55 $\mathrm{cm^{-1}}$处的弱吸收线，得到有效反射率$R_{\mathrm{eff}}=0.999\,3$，对应有效吸收光程为$L_{\mathrm{eff}}=d/(1-R_{\mathrm{eff}})=512$ m。

在WM-OA-ICOS中，由式(5)知，在腔内气体条件已知时，谐波信号大小与调制系数有关，即与调制幅度有关。实验中对不同调制振幅下OH自由基信号进行探测，结果如图3所示，OH自由基$2f$信号值先增大后减小，其中最大信号对应的最优调制振幅约在165 mV。

在最佳调制振幅设置为165 mV条件下，WM-OA-ICOS探测OH自由基时，开启紫外灯光解O_3，可清晰观察到OH自由基生成，得到的OH自由基和相邻位置H_2O的$2f$信号如图4所示，OH自由基和H_2O的$2f$信号强度分别为3.07 mV和7.69 mV。

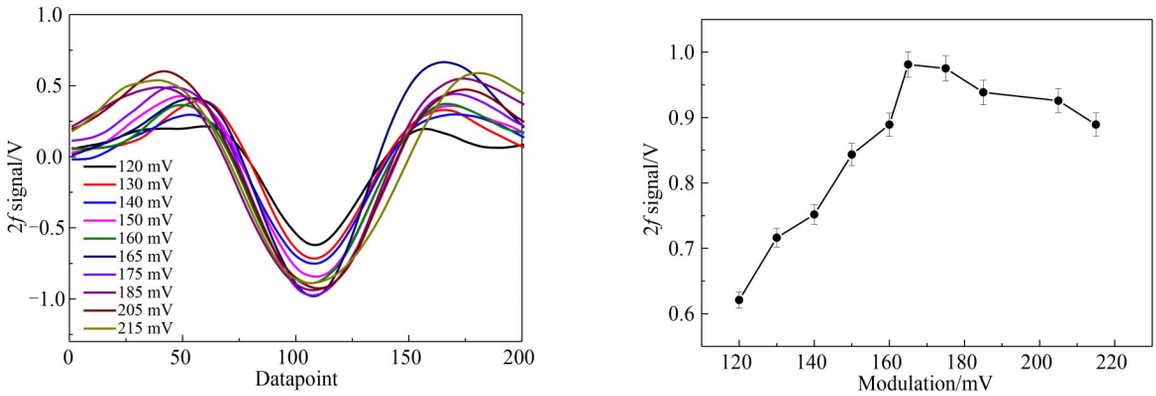

(a) The 2*f* signals of OH radicals with different amptitude　(b) The optimal modulation amptitude is 165 mV

图3　波长调制最优调制振幅

Fig. 3　The optimal modulation amptitude of WMS

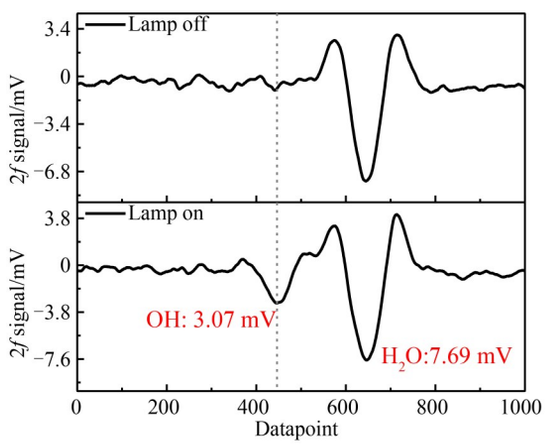

图4　紫外灯关闭或开启时OH自由基和相邻位置H_2O的2*f*信号

Fig. 4　The 2*f* signals of OH radicals and H_2O when the UV lamp turns off or on

通过腔内H_2O的浓度间接计算的方法，可得到光腔内OH自由基的绝对浓度为[44-45]

$$N_{OH}=\frac{2f_{OH}/I_{OH}}{2f_{H_2O}/I_{H_2O}}\frac{S_{H_2O}}{S_{OH}}N_{H_2O} \tag{8}$$

式中，N_{OH}和N_{H_2O}分别表示OH自由基和H_2O的分子数浓度，$2f_{OH}$和$2f_{H_2O}$为3 568.52 cm^{-1}处OH自由基和3 568.55 cm^{-1}处H_2O的2*f*信号强度，I_{OH}和I_{H_2O}分别为OH自由基和H_2O在吸收峰处对应的光强，S_{OH}和S_{H_2O}分别为OH自由基和H_2O的吸收线强，在296 K温度时分别为$S_{OH}=9.032\times10^{-20}\ cm^{-1}/(molecule\times cm^{-2})$和$S_{H_2O}=2.312\times10^{-26}\ cm^{-1}/(molecule\times cm^{-2})$[32]。$H_2O$的绝对浓度选择3 568.68 cm^{-1}处的直接吸收计算得到，即$N_{H_2O}=3.50\times10^{16}$ molecule/cm^3，其在296 K时的吸收线强为$3.990\times10^{-24}\ cm^{-1}/(molecule\times cm^{-2})$[32]。根据式(7)可以得到OH自由基浓度为$3.57\times10^9$ molecule/cm^3，此时其2*f*信号值为3.07 mV时。2*f*信号值与浓度呈现了很好的线性关系，如图5所示，关系式为

$$y=-7.59\times10^8+1.25\times10^8x \tag{9}$$

即1 mV二次谐波信号对应1.25×10^9 molecule/cm^3的OH自由基浓度，线性相关度为0.999 4。在后续进行OH自由基探测时，通过测量2*f*信号值，便能直接实时得到对应的OH自由基浓度。

OH自由基的探测极限利用2*f*信号无吸收处基线的标准偏差来评估。扫描频率为10 Hz，1 000次扫描平均，即采样时间为100 s时，基线波动标准差如图6所示为0.12 mV，此时OH的2*f*值为4.48 mV，因此OH自由基探测信噪比为38。根据式(9)得到$N_{OH}=4.84\times10^9$ molecule/cm^3，对应的OH自由基探测极限为1.2×10^8 molecule/cm^3(1σ，100 s)。

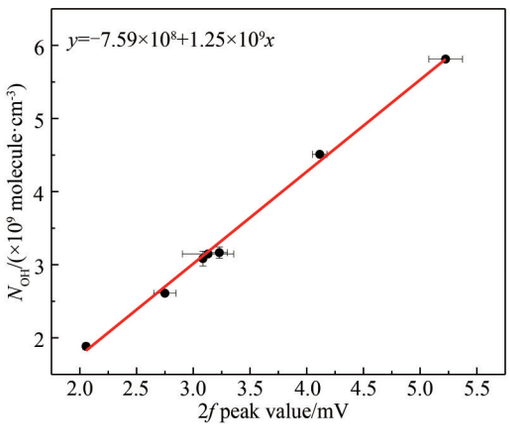

图5 OH自由基浓度与2*f*信号值的关系

Fig.5 OH radical concentrations versus 2*f* signal intensities

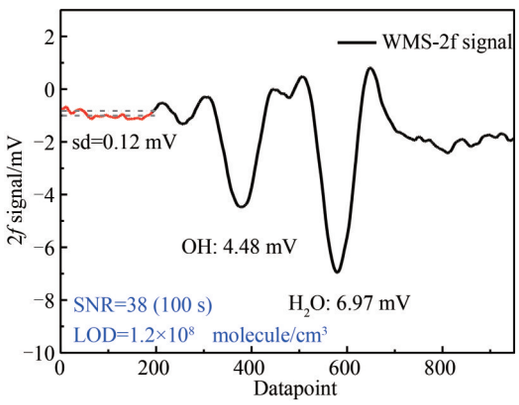

图6 OH自由基探测极限评估

Fig.6 Evaluation of the detection limit of OH radicals

4 结论

选择中红外2.8 μm DFB激光器作为光源，搭建了一套基于WM-OA-ICOS技术的装置，并将其应用于OH自由基探测。在512 m的有效光程和100 s平均时间下，系统的OH自由基探测限为1.2×10^{8} molecule/cm^{3}。实验研究表明，在低透过光强的离轴积分腔系统中，ASE强度由于不参加光腔的共振作用直接透过光腔而占据透过光强的大部分，对吸收产生极大影响。在光路上放置滤光片后，光强虽仅为原来的百分之几，但归一化的吸收显著提升约70倍。研究结果可为OH自由基直接探测提供新手段。

参考文献

[1] ENGELN R, BERDEN G, PEETERS R, et al. Cavity enhanced absorption and cavity enhanced magnetic rotation spectroscopy[J]. Review of Scientific Instruments, 1998, 69(11): 3763-3769.

[2] O'KEEFE A, DEACON D. Cavity ring-down optical spectrometer for absorption measurements using pulsed laser sources [J]. Review of Scientific Instruments, 1988, 59(12): 2544-2551.

[3] O'KEEFE A. Integrated cavity output analysis of ultra-weak absorption[J]. Chemical Physics Letters, 1998, 293(5-6): 331-336.

[4] O'KEEFE A, SCHERER J J, PAUL J B. Cw Integrated cavity output spectroscopy[J]. Chemical Physics Letters, 1999, 307(5-6): 343-349.

[5] PAUL J B, LAPSON L, ANDERSON J G. Ultrasensitive absorption spectroscopy with a high-finesse optical cavity and off-axis alignment[J]. Applied Optics, 2001, 40(27): 4904-4910.

[6] BAER D S, PAUL J B, GUPTA M, O'KEEFE A. Sensitive absorption measurements in the nearinfrared region using off-axis integrated cavityoutput spectroscopy[J]. Applied Physics B, 2002, 75(2-3): 261-265.

[7] WANG J J, TIAN X, DONG Y, et al. Enhancing off-axis integrated cavity output spectroscopy (OA-ICOS) with radio frequency white noise for gas sensing.[J]. Optics Express, 2019, 27(21):30517-30529.

[8] MSHESH P, SREENIVAS G, RAO P V N, et al. High-precision surface-level CO_2 and CH_4 using off-axis integrated cavity output spectroscopy (OA-ICOS) over Shadnagar, India[J]. International Journal of Remote Sensing, 2015, 36(21-22): 5754-5765.

[9] LIU Zidi, ZHENG Kaiyuan, ZHANG Haipeng, et al. Off-axis integrated cavity-enhanced infrared laser carbon dioxide sensor system[J]. Acta Photonica Sinica, 2020, 49(11): 1149014.
刘梓迪，郑凯元，张海鹏，等. 离轴积分腔增强红外激光二氧化碳传感系统[J]. 光子学报, 2020, 49(11): 1149014.

[10] SILVA M L, SONNENFROH D M, ROSEN D I, et al. Integrated cavity output spectroscopy measurements of NO levels in breath with a pulsed room-temperature QCL[J]. Applied Physics B, 2005, 81(5): 705-710.

[11] AZHAR M, MANDON J, NEERINCX, et al. A widely tunable, near-infrared laser-based trace gas sensor for hydrogen cyanide (HCN) detection in exhaled breath[J]. Applied Physics B, 2017, 123(11): 268.

[12] WITINSKI M F, SAYRES D S, ANDERSON J G. High precision methane isotopologue ratio measurements at ambient mixing ratios using integrated cavity output spectroscopy[J]. Applied Physics B, 2011, 102(2): 375-380.

[13] KASYUTICH V L, CANOSA-MAS C E, PFRANG C, et al. Off-axis continuous-wave cavity-enhanced absorption spectroscopy of narrow-band and broadband absorbers using red diode lasers[J]. Applied Physics B, 2002, 75(6-7): 755-761.

[14] ZYBIN A, KURITSYN Y A, MIRONENKO V R, et al. Cavity enhanced wavelength modulation spectrometry for application in chemical analysis[J]. Applied Physics B, 2004, 78(1): 103-109.
[15] BAKHIRKIN Y A, KOSTEREV A A, ROLLER C, et al. Mid-infrared quantum cascade laser based off-axis integrated cavity output spectroscopy for biogenic nitric oxide detection[J]. Applied Optics, 2004, 43(11): 2257-2266.
[16] BAKHIRKIN Y A, KOSTEREV A A, CURL R F, et al. Sub-ppbv nitric oxide concentration measurements using cw thermoelectrically cooled quantum cascade laser-based integratedcavity output spectroscopy[J]. Applied Physics B, 2006, 82(1): 149-154.
[17] ZHAO W X, GAO X M, CHEN W D, et al. Wavelength modulated off-axis integrated cavity output spectroscopy in the near infrared[J]. Applied Physics B, 2007, 86(2): 353-359.
[18] WU Tao, XU Dong, HE Xingdao, et al. Off-axis integrated cavity output spectroscopy technique based on wavelength modulation[J]. Acta Optica Sinica, 2017, 37(8): 389-398.
吴涛, 徐冬, 何兴道, 等.基于波长调制的离轴积分腔输出光谱技术[J].光学学报, 2017, 37(8): 389-398.
[19] MONKS P S. Gas-phase radical chemistry in the troposphere[J]. Chemical Society Reviews, 2005, 34(5): 376-395.
[20] CARSLAW N, CARSLAW D. The gas-phase chemistry of urban atmosphere[J]. Surveys in Geophysics, 2001, 22(1): 31-53.
[21] STON D, WHALLEY L K, HEARD D E. Tropospheric OH and HO_2 radicals: field measurements and model comparisons[J]. Chemical Society Reviews, 2012, 41(19): 6348.
[22] LELIEVELD J, BUTLER T M, CROWLEY J N, et al. Atmospheric oxidation capacity sustained by a tropical forest [J]. Nature, 2008, 452(7188): 737-740.
[23] RICKLY P, STEVENS P S. Measurements of a potential interference with laser-induced fluorescence measurements of ambient OH from the ozonolysis of biogenic alkenes[J]. Atmospheric Measurement Techniques, 2017, 11(1): 1-16.
[24] HAUSMANN M, BRANDENBURGER U, BRAUERS T, et al. Simple Monte Carlo methods to estimate the spectra evaluation error in differential-optical-absorption spectroscopy[J]. Applied Optics, 1999, 38(3): 462-475.
[25] YANG N N, FANG B, ZHAO W X, et al. Optical-feedback cavity-enhanced absorption spectroscopy for OH radical detection at 2.8 μm using a DFB diode laser[J]. Optics Express, 2022, 30(9): 15238-15249.
[26] MALARA P, MADDALONI P, GAGLIARDI G, et al. Combining a difference-frequency source with an off-axis high-finesse cavity for trace-gas monitoring around 3 μm[J]. Optics Express, 2006, 14(3): 1304-1313.
[27] FIEDLER S E, HESE A, RUTH A A. Incoherent broad-band cavity-enhanced absorption spectroscopy[J]. Chemical Physics Letters, 2003, 371(3): 284-294.
[28] TAN Z Q, LONG X W, FENG X W, et al. The study of wavelength modulation off-axis integrated cavity output spectroscopy in the case of Lorentzian absorption profile[J]. Optics Communications, 2011, 284(3): 852-856.
[29] KLUCZYNSKI P, GUSTAFSSON J, LINDBERG A M, et al. Wavelength modulation absorption spectrometry-an extensive scrutiny of the generation of signals[J]. Spectrochimica Acta, Part B. Atomic Spectroscopy, 2001, 56(8): 1277-1354.
[30] DING Wuwen, SUN Liqun, YI Luying. High sensitive scheme for methane remote sensor based on tunable diode laser absorption spectroscopy[J]. Acta Physica Sinica, 2017, 66(10): 53-61.
丁武文,孙利群,衣路英.基于可调谐半导体激光器吸收光谱的高灵敏度甲烷浓度遥测技术[J].物理学报,2017,66(10):53-61.
[31] CHEN Hao, JU Yu, HAN Li. Research on the relationship between modulation depth and center of high order harmonic in TDLAS wavelength modulation method[J]. Spectroscopy and Spectral Analysis, 2021, 41(12): 3676-3681.
陈昊,鞠昱,韩立. TDLAS波长调制法中调制深度与高次谐波中心幅值关系的研究[J].光谱学与光谱分析, 2021, 41(12): 3676-3681.
[32] GORDON I E, ROTHMAN L S, HARGREAVES R J, et al. The HITRAN2020 molecular spectroscopic database[J]. Journal of Quantitative Spectroscopy and Radiative Transfer, 2022, 277: 107949.
[33] NILLSON E J K, ESKEBJERG C, JOHNSON M S. A photochemical reactor for studies of atmospheric chemistry[J]. Atmospheric Environment, 2009, 43(18): 3029-3033.
[34] GUO Guangcan. Some physical problems of amplified spontaneous emission[J]. Physics, 1982, 10: 593-596.
郭光灿. 放大的自发辐射的若干物理问题[J]. 物理, 1982, 10: 593-596.
[35] 周炳坤, 高以智, 陈倜嵘, 等. 激光原理(第6版)[M]. 北京: 国防工业出版社, 2014.
[36] NADEZHDINSKII A I. Diode laser spectroscopy: precise spectral line shape measurements[J]. Spectrochimica Acta Part A, 1996, 52(8): 1041-1060.
[37] WELDON V, MCINERNEY D, PHELAN R, et al. Characteristics of several NIR tuneable diode lasers for spectroscopic based gas sensing: a comparison[J]. Spectrochim Acta A, 2006, 63(5): 1013-1020.
[38] KASYUTICH V L, MARTIN P A, HOLDSWORTH R J. An off-axis cavity-enhanced absorption spectrometer at 1 605 nm for the $^{12}CO_2/^{13}CO_2$ measurement[J]. Applied Physics B, 2006, 85(2-3): 413-420.

[39] ROMANINI D, LEHMANN K K. Ring-down cavity absorption spectroscopy of the very weak HCN overtone bands with six, seven, and eight stretching quanta[J]. The Journal of Chemical Physics, 1993, 99(9): 6287-6301.
[40] HELDEN J H, SCHRAM D C, ENGELN R. Phase-shift cavity ring-down spectroscopy to determine absolute line intensities[J]. Chemical Physics Letters, 2004, 400(4-6): 320-325.
[41] KASYUTICH V L, MARTIN P A, HOLDSWORTH R J. Effect of broadband amplified spontaneous emission on absorption measurements in phase-shift off-axis cavity enhanced absorption spectroscopy[J]. Chemical Physics Letters, 2006, 430(4-6):429-434.
[42] KASYUTICH V L, MARTINP A. On quantitative measurements in phase-shift off-axis cavity-enhanced absorption spectroscopy[J]. Chemical Physics Letters, 2007, 446(1-3):206-211.
[43] ZHAO W X, GAO X M, DENG L H, et al. Absorption spectroscopy of formaldehyde at 1.573 μm[J]. Journal of Quantitative Spectroscopy & Radiative Transfer, 2007, 107(2): 331-339.
[44] GUAN Mengxue, CHEN Daqiang, HU Shiqi, et al. Theoretical insights into ultrafast dynamics in quantum materials[J]. Ultrafast Science, 2022, 2022:9767251.
[45] ZHAO W X, FANG B, LINX X, et al. Superconducting-magnet-based faraday rotation spectrometer for real time in situ measurement of OH radicals at 10^6 molecule/cm^3 level in an atmospheric simulation chamber[J]. Analytical Chemistry, 2018, 90(6): 3958-3964.

Wavelength Modulation Off-axis Integrated Cavity Output Spectroscopy for High-sensitivity Detection of OH Radicals in Mid-infrared

YANG Nana[1,2], FANG Bo[1], WANG Chunhui[1,3], ZHOU Hao[1,2], WEI Nana[1], ZHAO Weixiong[1], ZHANG Weijun[1,3]

(1 *Anhui Institute of Optics and Fine Mechanics, HFIPS, Chinese Academy of Sciences, Hefei* 230031, *China*)
(2 *University of Science and Technology of China, Hefei* 230026, *China*)
(3 *School of Environmental Science and Optoelectronic Technology, University of Science and Technology of China, Hefei* 230026, *China*)

Abstract: The hydroxyl (OH) free radical is one of the most important oxidants and is at the origin of the majority of chemical transformations in the troposphere. It plays a key role in the formation of ozone and secondary organic aerosols. Accurate and quantitative measurements of OH radical is of great significance to atmospheric chemistry research and air quality control. However, due to the low concentrations in the atmosphere (~10^6 molecule/cm^3), high reactivity, and very short lifetime (<1 s), current techniques that can be successfully employed for tropospheric OH measurement are extremely limited. Therefore, there is a strong driving force for the development of new techniques. Off-axis Integrated Cavity Output Spectroscopy (OA-ICOS) based on Lambert-Beer law can offer an ultra-long optical pathlength on the order of kilometers utilizing a high-finesse optical resonator with a limited optical base length. In addition, the off-axis paths through optical cavity can actively excite higher-order transverse modes and effectively reduce the influence of cavity mode fluctuation. These advantages make it a powerful tool for sensitive measurement of OH radical. We reported the development of a mid-infrared OA-ICOS experimental setup. A room temperature continuous-wave distributed feedback diode laser emitting at 2.8 μm was used as the probe laser. The Q(1.5e) transition line of OH radical located at 3 568.52 cm^{-1} was selected for detection. The integrated cavity consisted of two 25.4-mm diameter high-reflectivity dielectrically coated plano-concave mirrors (1 m radius of curvature) separated by a distance of 35.8 cm. The measured effective reflectivity of the cavity mirrors was 0.999 3, corresponding to the effective optical path of 512 m. In this mid-infrared OA-ICOS system, the amplified spontaneous emission of the distributed feedback laser, which is usually on the order of nanowatts and is a kind of unwanted broadband radiation outside the highly reflective band of the cavity mirrors, directly passed through the cavity without resonating. This amplified spontaneous emission was received by the detector together with the weak valid absorption signal, causing interference in measurement. It was found that the absorption was about 70 times underestimated due to the amplified spontaneous emission, which needs to be effectively avoided. To reduce the $1/f$ noise and improve the sensitivity of this system, wavelength modulation spectroscopy was

applied. The laser current was swept and modulated by a triangle wave and a sinusoidal wave around the absorption peak to obtain the second harmonic ($2f$) signals. The sample of OH radical were generated by the reaction of H_2O and $O(^1D)$ produced by O_3 photolysis. The concentration of OH in the cavity was determined by a reference absorption line of H_2O in the same spectral region at 3 568.55 cm^{-1} whose concentration could be calculated by direct absorption spectroscopy. The strong linear relationship (correlation coefficient of 0.999 4) between $2f$ signals and concentrations was exhibited. Based on a typical spectrum measured under an OH concentration of 4.84×10^9 molecule/cm^3 and 100 s data acquisition time, the noise level was evaluated by standard deviation from the non-absorption wing, giving a signal-to-noise ratio of about 38. From these results, the detection limit of OH radical was determined to be 1.2×10^8 molecules/cm^3 (1σ). The performance of this spectrometer can be further improved by reducing the residual cavity resonances, using higher reflectivity cavity mirrors to increase the absorption path length and signal intensity, re-injecting to the cavity via a third mirror and improving the effective gain of the detector. In particular, the Wavelength Modulation Off-axis Integrated Cavity Output Spectroscopy (WM-OA-ICOS) technique in the mid-infrared provides a new direct spectral method for OH radical detection. The successful combination of OA-ICOS and wavelength modulation spectroscopy means that OA-ICOS also can be combined further with other modulation technologies, such as frequency modulation spectroscopy, to achieve shot-noise limited detection.

Key words: Laser absorption spectroscopy; Mid-infrared; Off-axis integrated cavity; Amplified spontaneous emission; OH radical

OCIS Codes: 140.3600; 300.1030; 300.6360; 300.6340

Foundation item: National Natural Science Foundation of China (Nos. 42022051, 41627810), the Youth Innovation Promotion Association CAS (No.Y202089), the HFIPS Director's Fund (Nos.YZJJ202101, BJPY2019B02)